


RESEARCH PAPER



Tricyclic coumarin sulphonate derivatives with alkaline phosphatase inhibitory effects: *in vitro* and docking studies

Jamshed Iqbal^{a*}, Mohammed I. El-Gamal^{b,c,d*} , Syeda Abida Ejaz^a, Joanna Lecka^{e,f}, Jean Sévigny^{e,f} and Chang-Hyun Oh^{g,h}

^aCentre for Advanced Drug Research, COMSATS Institute of Information Technology, Abbottabad, Pakistan; ^bDepartment of Medicinal Chemistry, College of Pharmacy, University of Sharjah, Sharjah, United Arab Emirates; ^cSharjah Institute for Medical Research, University of Sharjah, Sharjah, United Arab Emirates; ^dDepartment of Medicinal Chemistry, University of Mansoura, Mansoura, Egypt; ^eDépartement de microbiologie-infectiologie et d'immunologie, Faculté de Médecine, Université Laval, Québec, Canada; ^fCentre de Recherche du CHU de Québec, Université Laval, Québec, Canada; ^gCenter for Biomaterials, Korea Institute of Science and Technology, Seoul, Republic of Korea; ^hDepartment of Biomolecular Science, University of Science and Technology, Daejeon, Republic of Korea

ABSTRACT

Tissue-nonspecific alkaline phosphatase (TNAP) is an important isozyme of alkaline phosphatases, which plays different pivotal roles within the human body. Most importantly, it is responsible for maintaining the balanced ratio of phosphate and inorganic pyrophosphate, thus regulates the extracellular matrix calcification during bone formation and growth. The elevated level of TNAP has been linked to vascular calcification and end-stage renal diseases. Consequently, there is a need to search for highly potent and selective inhibitors of alkaline phosphatases (APs) for treatment of disorders associated with the over-expression of APs. Herein, a series of tricyclic coumarin sulphonate **1a-za** with known antiproliferative activity, was evaluated for AP inhibition against human tissue nonspecific alkaline phosphatase (*h*-TNAP) and human intestinal alkaline phosphatase (*h*-IAP). The methylbenzenesulphonate derivative **1f** ($IC_{50} = 0.38 \pm 0.01 \mu M$) was found to be the most active *h*-TNAP inhibitor. Another 4-fluorobenzenesulphonate derivative **1i** ($IC_{50} = 0.45 \pm 0.02 \mu M$) was found as the strongest inhibitor of *h*-IAP. Some of the derivatives were also identified as highly selective inhibitors of APs. Detailed structure-activity relationship (SAR) was investigated to identify the functional groups responsible for the effective inhibition of AP isozymes. The study was also supported by the docking studies to rationalise the most possible binding site interactions of the identified inhibitors with the targeted enzymes.

ARTICLE HISTORY

Received 12 December 2017
Revised 11 January 2018
Accepted 11 January 2018

KEYWORDS



Alkaline phosphatase inhibitor; coumarin; molecular docking; structure-activity relationship; Tricyclic coumarin sulfonate

Introduction


Alkaline phosphatases (APs, E.C. 3.1.3.1) are membrane-bound ecto-enzymes with an extracellular-oriented active site¹. They belong to the large family of ecto-enzyme known as ecto-nucleotidases, and are involved in various physiological functions within the human body, most importantly in phosphorylation and dephosphorylation reactions². They are also responsible for the hydrolysis and breakdown of wide variety of nucleoside tri- and di-phosphates substrates to their respective monophosphates^{3,4}. They also hydrolyse many other phosphate-containing substrates, such as inorganic pyrophosphate (PPi), glucose phosphate, polyphosphates, phosphomonoesters, and phosphatidates⁵. APs are further categorised into two types, the tissue-specific and tissue-nonspecific alkaline phosphatases (TNAPs). From the tissue-specific AP type, intestinal alkaline phosphatase (IAP) plays a pivotal role in the maintenance of physiological environment of the intestine⁶. Moreover, this isozyme is important for the regulation of bicarbonate secretion balance, duodenal luminal pH, dephosphorylation reaction, and helps in the maintenance of normal gut environment

by detoxifying the bacterial toxins⁷. TNAP is widely distributed almost in each body part but is abundantly present in central nervous tissues, mineralising tissues and also in kidney⁸. As compared to the other body tissues, high concentration of TNAP is present in the mineralising tissues such as teeth and bones for the normal teeth and bone formation. But too high concentrations of TNAP in mineralising tissue results in abnormal calcification and mineral deposition⁹. The identification of effective inhibitors of AP isozymes becomes an emerging drug target for the disorders related to the hyper-activity of TNAP and IAP. To date, different inhibitors of APs based on triazole, pyrazoles, coumarin sulphonates, diaryl sulphonamides, and chromones have been identified as effective inhibitors of TNAP and IAP (Figure 1)¹⁰⁻¹³.

Recently, we have reported coumarinyl sulphonates derivatives as novel and potent inhibitors of *h*-TNAP and *h*-IAP¹³. In continuation of our efforts for searching the effective and selective inhibitors, herein we evaluated a series of 27 tricyclic-fused coumarin sulphonate derivatives **1a-za** as inhibitors of APs which were already tested for their antiproliferative and anti-inflammatory activities¹⁴⁻¹⁷. We assumed that the fused cycloheptane or cyclooctane

CONTACT Chang-Hyun Oh  choh@kist.re.kr  Center for Biomaterials, Korea Institute of Science and Technology, PO Box 131, Cheongryang, Seoul 130-650, Republic of Korea

*These authors contributed equally to this work.

 Supplemental data for this article can be accessed [here](#).

© 2018 The Author(s). Published by Informa UK Limited, trading as Taylor & Francis Group.

This is an Open Access article distributed under the terms of the Creative Commons Attribution License (<http://creativecommons.org/licenses/by/4.0/>), which permits unrestricted use, distribution, and reproduction in any medium, provided the original work is properly cited.

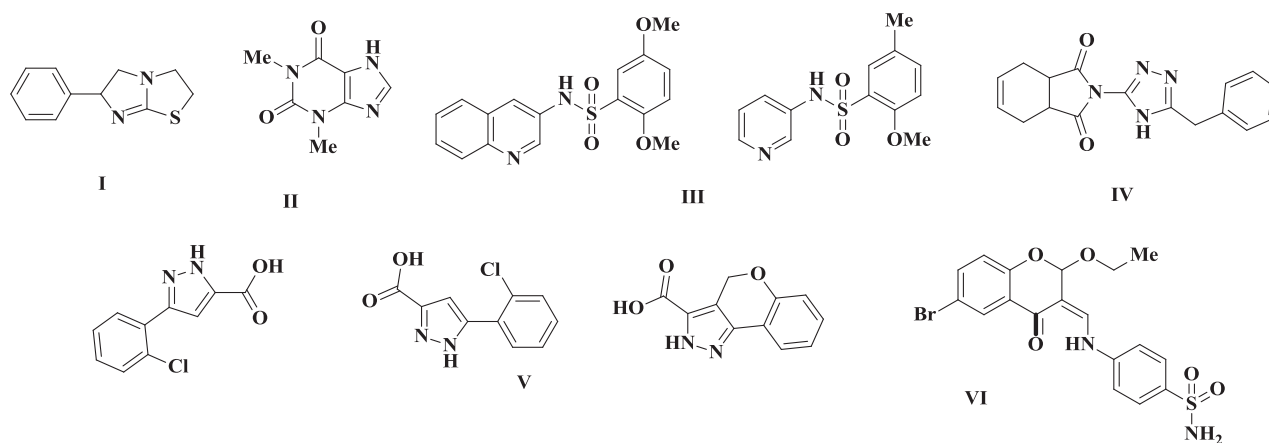


Figure 1. APs inhibitors; (I) Levamisole (II) Theophylline (III) Aryl sulphonamide-based inhibitors (IV) trizole-based inhibitors (V) Pyrazole-based Inhibitors, (VI) coumarinyl sulphonates.

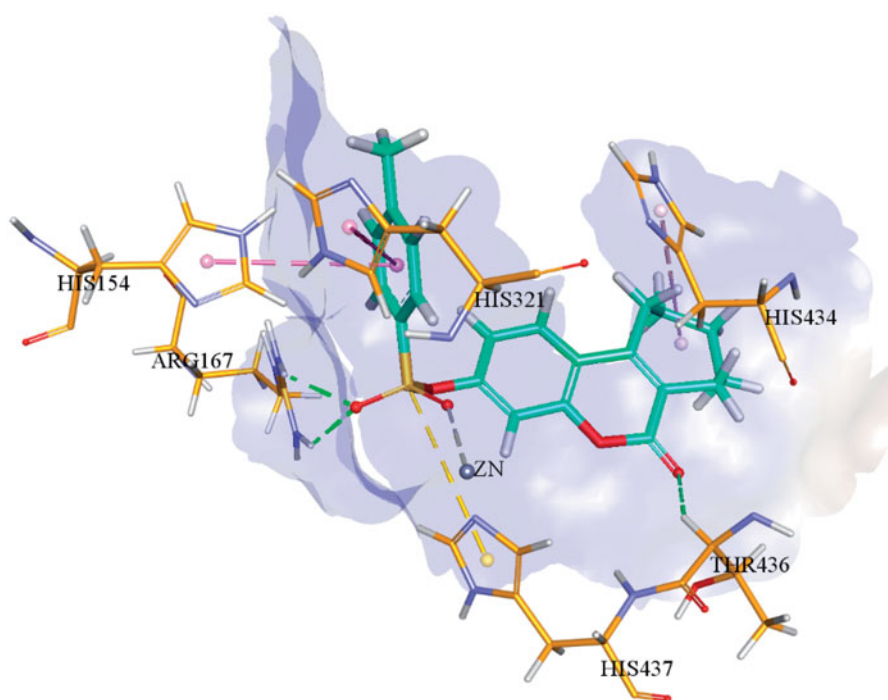


Figure 2. 3D binding interactions of most potent inhibitor **1f** within the active site of *h*-TNAP. Hydrogen bonds are shown in green dotted line while π - π interactions are shown in purple dotted line.

ring might contribute to stronger affinity than the previously reported bicyclic coumarin sulphonate derivatives through formation of additional hydrophobic interaction(s). Our assumption succeeded as shown in [Figure 2](#). Except two derivatives **1w** and **1y**, all the other compounds were found as effective AP inhibitors with sub-micromolar or very low micro-molar range IC_{50} values. Further, the most effective inhibitors of either *h*-TNAP or *h*-IAP were selected for the molecular docking studies to rationalise the possible binding interactions with the respective targeted enzymes.

Experimental

Synthesis of the target molecules **1a-z**

The synthetic procedures, purification methods, and the spectral analysis data have been reported^{14–17}. The experimental details as well as representative analysis charts are provided in the [supplementary file](#).

Bioactivity protocol

Alkaline phosphatase inhibition assay (*h*-TNAP and *h*-IAP)

The inhibition assay was performed by following the already reported method¹⁸ and the inhibitory activity was measured at the final concentration of 200 μ M in diethanolamine (DEA) buffer as discussed in our published article¹⁹. The first step of the inhibition assay was the treatment of 10 μ l of tested derivatives with 20 μ l of *h*-TNAP (46 ng/well) or of *h*-IAP (57 ng/well). The plates were incubated at 37 °C for 5–10 min, and luminescence signals were recorded by microplate reader (BioTek FLx800, Instruments, Inc., Winooski, VT). Then, 20 μ l of CDP-star[®] substrate was added to each reaction mixture and signals were again measured as after-read, after 15–20 min of incubation. The data were scrutinised by PRISM 5.0 (GraphPad, San Diego, CA) software and the inhibitory concentration values (IC_{50} values) were attained as discussed earlier.

Molecular docking studies

Molecular docking studies of compounds **1f** and **1i**, potent inhibitors of *h*-TNAP and *h*-IAP, respectively, were conducted to investigate the probable binding interactions of these compounds within the active site of the respective target enzyme. Our previously reported models of *h*-TNAP and *h*-IAP were used for docking calculation²⁰. Before performing docking studies, protonation and energy minimisation of all enzyme structures were carried out using molecular operating environment (MOE) 2014, 09 software²¹. Structure generation as well as energy minimisation of the effective inhibitors were also carried out via MOE software. After preparation of all the prerequisite compounds and enzymes structures, total 50 independent docking runs for each ligand were executed by MOE docking program. The best scored pose of potent compounds in each target enzyme was selected for evaluation of binding interactions. Binding free energy for each pose was also determined and pose with the lowest free binding energy was selected for further visualisation studies. 3D visualisation of binding interaction between potent compound and respective target was carried out using Discovery studio visualizer v4²².

Results and discussion

Chemistry

Scheme 1 illustrates the synthetic pathway via which the target compounds **1a-za** were prepared. Cycloheptanone (**2a**) or cyclooctanone (**2b**) was reacted with diethyl carbonate in the presence of NaH in benzene at the reflux temperature to get the ester intermediates **3a,b** that exist in keto-enol tautomers²³. Subsequent reaction with (substituted) resorcinol in the presence of trifluoroacetic acid and concentrated sulphuric acid led to the production of the tricyclic phenolic intermediates **4a-f**²⁴. They were used in the next step as such with no prior purification. In the last step, those phenolic intermediates were treated with the appropriate sulphonyl chloride reagent in the presence of triethylamine as a catalyst to get the target sulphonate products **1a-za**¹⁴⁻¹⁷. Table 1 illustrates the structure of each target compound.

Alkaline phosphatase inhibition

All synthesised tricyclic coumarin sulphonate derivatives **1a-za** were tested for their potential to inhibit *h*-TNAP and *h*-IAP. Except two compounds (**1w** and **1y**), all compounds were found to be active against both isozymes of AP with IC₅₀ values in the lower micro-molar range. Compounds showed their *h*-TNAP inhibitory

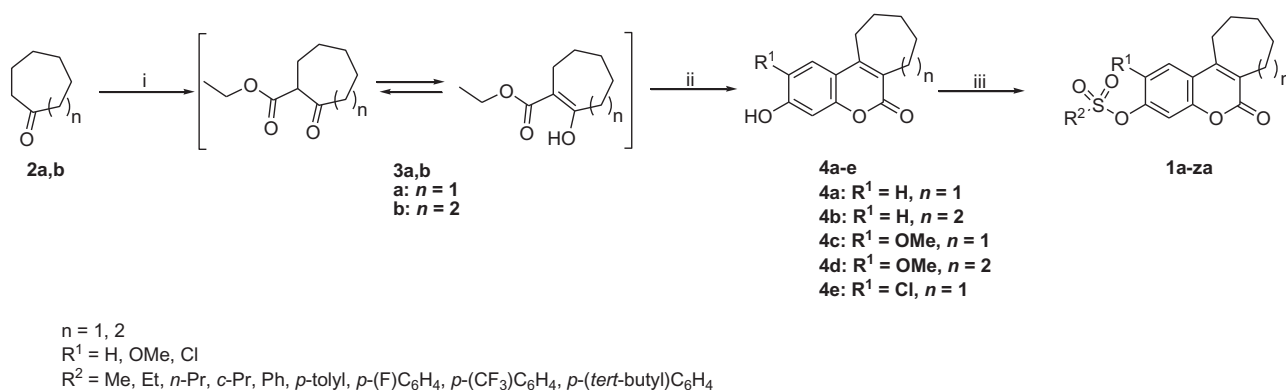
potential in the range of IC₅₀ = 0.38 ± 0.01 to 8.57 ± 0.73 μM as compared to standard levamisole (IC₅₀ = 20.21 ± 1.9 μM), and *h*-IAP inhibitory activity in the range of IC₅₀ = 0.45 ± 0.09 to 11.8 ± 1.91 μM as compared to standard L-phenylalanine (IC₅₀ = 100.1 ± 3.15 μM) (Table 1).

Structure-activity relationship (SAR)

In order to find out the comprehensive structure-activity relationship for AP inhibition, all tricyclic-fused coumarin sulphonates **1a-za** were divided into two categories, on the basis of fused cycloheptane and cyclooctane ring. Moreover, the detailed structure-selectivity relationship was also rationalised on the basis of effect of unsubstituted, and chloro- and methoxy-substituted derivatives on the inhibition of both APs. Compounds **1q** and **1z** were found as selective inhibitors of *h*-TNAP while none of the derivative was found as a selective inhibitor of IAP.

Among the tested derivatives, compound **1f** expressed maximum inhibitory effects on *h*-TNAP and compound **1i** depicted the strongest potency against *h*-IAP. From the unsubstituted derivatives, except compound **1c**, **1g**, and **1m**, the other target derivatives expressed varying inhibitory effects on *h*-TNAP. Compounds **1f**, **1a**, and **1d** possessing *p*-toluene sulphonate, methane sulphonate, and cyclopropane substitution, respectively, depicted higher inhibition of *h*-TNAP than compounds **1c**, **1g**, and **1j-m**. Among the cyclooctane-fused derivatives, compound **1l** with benzenesulphonate substitution demonstrated the strongest inhibitory potential on *h*-TNAP (IC₅₀ ± SEM = 1.13 ± 0.21 μM). Compounds **1c** with the fused cycloheptane ring and compound **1j** with the fused cyclooctane ring were found as stronger inhibitors of *h*-IAP with the inhibitory values of IC₅₀ ± SEM = 0.91 ± 0.06 and 0.84 ± 0.09 μM, respectively. Among the cyclooctane-fused derivatives, compound **1j** with ethanesulphonate substitution demonstrated the strongest inhibitory effect on *h*-IAP (IC₅₀ ± SEM = 0.84 ± 0.09 μM). From the cycloheptane-fused derivatives, compound **1c** with propanesulphonate substitution demonstrated the strongest inhibitory potential on *h*-IAP (IC₅₀ ± SEM = 0.91 ± 0.06 μM). Although more lipophilic side chain was substituted in **1c**, the inhibitory effect of this derivative was found less because of the presence of seven-membered fused ring. Moreover, from the obtained results this may be rationalised that the presence of more lipophilic side chain in compound **1c** may form stronger hydrophobic interactions with the target enzyme.

The inhibitory effect by other derivatives; **1h** and **1n** with *tert*-butylbenzene sulphonate moiety expressed the dual inhibition of both isozymes of APs. The derivative **1n** depicted more inhibitory potential because of the presence of fused eight membered ring (*h*-TNAP;



Scheme 1. Reagents and conditions: (i) diethyl carbonate, NaH, benzene, reflux, 90% (**3a**, $n = 1$), 85% (**3b**, $n = 2$); (ii) (substituted) resorcinol, CF₃COOH, conc. H₂SO₄, 0 °C; rt, 3 h; (iii) appropriate sulphonyl chloride derivative, triethylamine, CH₂Cl₂, 0 °C; rt, 1 h.

Table 1. Structures of the target compounds **1a-za** along with their yield percentages and *in vitro* inhibitory effects (IC₅₀, μM) against *h*-TNAP and *h*-IAP.

Compound No.	R ¹	R ²	n	Yield%	IC ₅₀ (μM) ± SEM ^a	
					<i>h</i> -TNAP	<i>h</i> -IAP
1a	H	Me	1	95	0.48 ± 0.01	1.98 ± 0.19
1b	H	Et	1	92	2.13 ± 0.19	2.71 ± 0.23
1c	H	<i>n</i> -Pr	1	93	1.52 ± 0.17	0.91 ± 0.06
1d	H	Cyclo-Pr	1	85	0.98 ± 0.13	0.96 ± 0.08
1e	H	Ph	1	93	8.57 ± 0.73	1.84 ± 0.19
1f	H	<i>p</i> -Tolyl	1	95	0.38 ± 0.01	1.94 ± 0.11
1g	H	<i>p</i> -(CF ₃)C ₆ H ₄	1	90	1.59 ± 0.12	2.64 ± 0.45
1h	H	<i>p</i> -(<i>tert</i> -butyl)C ₆ H ₄	1	95	6.33 ± 0.99	3.92 ± 0.47
1i	H	<i>p</i> -(F)C ₆ H ₄	1	82	1.06 ± 0.11	0.45 ± 0.09
1j	H	Et	2	90	1.74 ± 0.14	0.84 ± 0.09
1k	H	<i>n</i> -Pr	2	88	1.91 ± 0.11	3.37 ± 0.79
1l	H	Ph	2	92	1.13 ± 0.21	2.82 ± 0.82
1m	H	<i>p</i> -Tolyl	2	95	1.59 ± 0.16	2.12 ± 0.23
1n	H	<i>p</i> -(<i>tert</i> -butyl)C ₆ H ₄	2	94	1.85 ± 0.13	1.28 ± 0.13
1o	OMe	Me	1	85	1.21 ± 0.11	11.80 ± 1.91
1p	OMe	Me	2	85	1.49 ± 0.13	1.51 ± 0.17
1q	OMe	<i>n</i> -Pr	1	95	4.31 ± 0.99	>100
1r	OMe	<i>n</i> -Pr	2	91	2.60 ± 0.49	0.75 ± 0.07
1s	OMe	Ph	1	92	1.26 ± 0.07	3.88 ± 0.32
1t	OMe	Ph	2	87	2.68 ± 0.18	0.83 ± 0.06
1u	OMe	<i>p</i> -Tolyl	1	96	1.65 ± 0.13	0.79 ± 0.05
1v	OMe	<i>p</i> -Tolyl	2	90	0.64 ± 0.02	1.45 ± 0.04
1w	OMe	<i>p</i> -(CF ₃)C ₆ H ₄	1	87	>100	>100
1x	OMe	<i>p</i> -(CF ₃)C ₆ H ₄	2	85	1.29 ± 0.12	1.63 ± 0.19
1y	Cl	Me	1	85	>100	>100
1z	Cl	Ph	1	85	5.73 ± 1.06	>100
1za	Cl	<i>p</i> -Tolyl	1	86	2.22 ± 0.27	1.11 ± 0.01
Levamisole	—	—	—	—	20.2 ± 1.90	—
L-Phenylalanine	—	—	—	—	—	100 ± 3.15

^aIC₅₀ is the concentration at which the 50% of the enzyme activity was inhibited. All the values were expressed as IC₅₀ ± SEM (standard error mean), *n* = 3.

IC₅₀ ± SEM = 1.85 ± 0.13 μM, *h*-IAP; IC₅₀ ± SEM = 1.28 ± 0.13 μM). In comparison to **1h**, the replacement of *tert*-butylbenzene with fluorobenzenesulphonate results in the most potent inhibitor of *h*-IAP i.e. **1i**. Compound **1i** was identified as the strongest inhibitor of *h*-IAP with an inhibitory value of IC₅₀ ± SEM = 0.45 ± 0.09 μM. The increased potency might be due to the presence of most electronegative halogen.

On the other hand, the chloro- and methoxy-substituted derivatives were found more active against both APs than the unsubstituted analogues. With reference to *h*-TNAP, compound **1o** (IC₅₀ ± SEM = 1.21 ± 0.11 μM) was found more potent as compared to compound **1q** (IC₅₀ ± SEM = 4.31 ± 0.99 μM), **1p** (IC₅₀ ± SEM = 1.49 ± 0.13 μM), and **1r** (IC₅₀ ± SEM = 2.60 ± 0.49 μM) but with reference to *h*-IAP, **1p** (IC₅₀ ± SEM = 1.51 ± 0.17 μM) was found more better than **1o** (IC₅₀ ± SEM = 11.8 ± 1.91 μM) and **1r** (IC₅₀ ± SEM = 0.75 ± 0.07 μM) was found better than **1q** (IC₅₀ ± SEM = >100 μM). It means that the presence of functional group is playing more important role on the inhibitory effects. The derivatives with less carbon number were found more potent than the propane derivative. But, with detailed SAR it was found that the heptane ring was favourable for TNAP, while octanone derivative was found potent towards IAP. When the activity of **1o** was compared with **1r** and **1p**, it was observed that the reduced inhibitory effect of both the derivatives on TNAP was due to the presence of *n*-propane substitution in case of **1r**, and the presence of fused cyclooctane ring in case of **1p**.

In comparison to **1o**, compound **1s** having benzenesulphonate substitution was found almost as an equipotent inhibitor of TNAP with the inhibitory value of 1.26 ± 0.07 μM. The other derivative

i.e. **1t** having the same substitution of benzenesulphonate as in compound **1s**, but with the cyclooctane ring, a reduced inhibitory effect on TNAP was observed with an increased inhibitory effect on IAP isozymes (*h*-TNAP; (IC₅₀ ± SEM = 2.68 ± 0.18 μM, *h*-IAP; IC₅₀ ± SEM = 0.83 ± 0.06 μM). The derivatives **1w** and **1x** having the same substitution at R¹ and R² positions but with cycloheptane and cyclooctane ring in **1w** and **1x**, respectively. When the SAR of these two derivatives was considered, it was observed that cycloheptane derivative **1w** was found less reactive than that of the cyclooctane derivative **1x** which inhibited both isozymes effectively. This inhibitory effect confirms that like **1p**, the presence of more carbon number in the derivative is responsible for the more inhibition.

An interesting inhibition of IAP was also exhibited by the aromatic derivative **1u** and **1za** processing cycloheptane ring along with *p*-tosylate substitution at R² position but different substitution at R¹ position. The derivative with electron-donating group i.e. OMe in case of **1u** (IC₅₀ ± SEM = 0.79 ± 0.05 μM) was found more active inhibitor as compared to the derivative **1za** (IC₅₀ ± SEM = 1.11 ± 0.01 μM) with electron-withdrawing substitution. These two derivatives also exert some inhibitory potential on *h*-TNAP, but less (**1u**; IC₅₀ ± SEM = 1.65 ± 0.13 μM, **1za**; IC₅₀ ± SEM = 2.22 ± 0.27 μM) in comparison to *h*-IAP. The other derivatives **1y** and **1z** with methanesulphonate and benzenesulphonate substitution were found inactive towards *h*-IAP. Moreover, it was found that the aromatic sulphonate derivatives **1s**, **1u**, and **1za** depicted stronger inhibitory effects on *h*-IAP than *h*-TNAP.

The results obtained here are in consistent with our previously reported work. The 2-methoxy- or 2-chloro- substituted derivatives

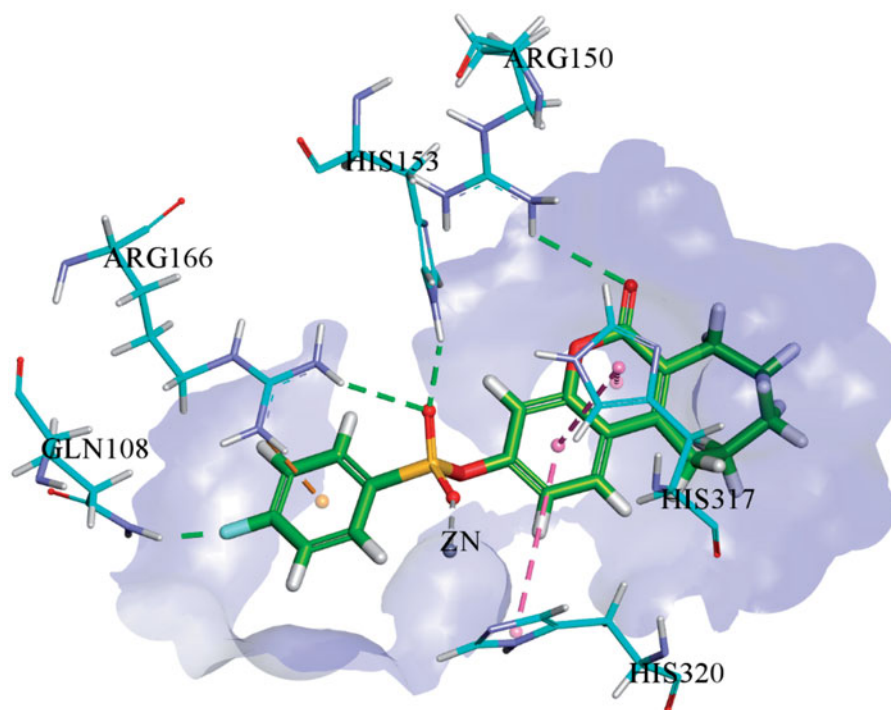


Figure 3. 3D binding interactions of most potent inhibitor **1i** within the active site of *h*-IAP. Hydrogen bonds are shown in green dotted line while π - π interactions are shown in purple dotted line.

possessing the fused cycloheptane ring were found stronger inhibitors of *h*-TNAP than the corresponding analogues having fused cyclooctane ring. Similarly, an inverse effect was observed towards *h*-IAP. It can be suggested from the obtained data that the derivatives with more lipophilic side chains led to the more inhibition of *h*-IAP and vice versa in case of *h*-TNAP. This lipophilic side chains might be involved in some hydrophobic interactions within the pocket of the receptor site and increase the affinity of such derivatives for the targeted enzyme and ultimately accounts for the enhanced *h*-IAP inhibition.

Molecular docking studies

Molecular docking studies of the most potent derivatives i.e. **1f** and **1i** were carried out within the respective target enzyme and their most probable binding interactions within the modelled enzymes are depicted in Figures 2 and 3. Detailed analysis of binding interaction of compound **1f** within *h*-TNAP revealed that oxygen atom in both sulphonate group and carbonyl group are responsible for making three strong hydrogen bonds with amino acid residues. Two hydrogen bonds were formed by oxygen of sulphonate group with amino groups of Arg167 while the third hydrogen bond was formed by carbonyl oxygen in coumarin ring with amino acid Thr436. Additional to hydrogen bonding, second oxygen atom of the sulphonate group also formed direct interaction with the Zn^{+2} ion within the active site of *h*-TNAP. The excellent *h*-TNAP inhibition activity of compound **1f** can be related with this direct binding interaction of sulphonate oxygen with the Zn^{+2} ion of the active site. Furthermore, two π - π interactions were formed by benzene ring adjacent to sulphonate group with amino acid residues His154 and His321. One π -alkyl interaction was also exhibited by the seven-membered ring fused with the coumarin ring and His434 as shown in Figure 2. This interaction may account for the stronger affinity and potency of this tricyclic compound compared to the previously reported bicyclic coumarin sulphonate derivatives¹³. Detailed binding interaction of **1i** with

h-IAP is shown in Figure 3. In comparison to docking interaction of compound **1f** with *h*-TNAP, compound **1i** formed four hydrogen bonds with different amino acids of *h*-IAP. Oxygen atom in sulphonate group of compound **1i** also formed two hydrogen and one metal interaction. These two hydrogen bonds were formed by one oxygen atom in sulphonate group with amino acid residue of Arg166 and His143. While other oxygen of sulphonate group formed interaction with Zn^{+2} ion. Carbonyl oxygen in coumarin ring and fluorine atom in compound **1i** also formed hydrogen bond with amino acid residues Arg150 and Gln108 as shown in Figure 3. Additional to hydrogen bonding, two π - π interaction were also formed by benzene ring of coumarin ring with amino acid residue of His317 and His320. Metal interaction of sulphonate group with metal ion is analogous to previously reported interaction of sulphonamides with different APs¹³. π -alkyl interaction between seven-membered ring adjacent to coumarin ring was not shown as in **1i**. Docking of the inactive derivatives **1q** and **1w** showed weaker affinity and fewer bonds formed, which supports the SAR discussion. The figures are given in the supplementary file.

Conclusions

Tricyclic-fused coumarin sulphonates **1a-za** were evaluated for their effective inhibitory potential against *h*-TNAP and *h*-IAP. Except **1w** and **1y** derivatives, all the other compounds exhibited excellent inhibitory potential against both *h*-TNAP and *h*-IAP. Methylbenzenesulphonate derivative **1f** ($IC_{50} = 0.38 \pm 0.01 \mu M$) was found to be the most active *h*-TNAP inhibitor. Another 4-fluorobenzenesulphonate derivative **1i** ($IC_{50} = 0.45 \pm 0.02 \mu M$) was found as the strongest inhibitor of *h*-IAP. Detailed SAR studies and molecular docking studies were performed to identify the importance of functional groups within the structures and to explore the possible binding site interactions, respectively. Moreover, previously these derivatives have been reported for their antiproliferative effects against different cell lines including, leukaemia, CNS,

prostate, renal, colon, lung cancer, melanoma, ovarian, and breast cancers. From that data we got **1i** and **1m** as the strongest anti-proliferative derivatives against colon cancer cell line along with the maximum anti-inflammatory effects. Here in this study, we have identified these compounds as stronger inhibitors of *h*-IAP isozymes. This can be rationalised that the IAP, responsible for the maintenance of intestinal homeostasis, might be over-expressed in the colon cancer cell lines. Moreover, the over-expression of *h*-TNAP can be associated with the lung cancer, melanoma, ovarian, breast cancers, and renal cancer. Therefore, the obtained results synergise with the previously reported data. It can be suggested that the potent inhibitors of both *h*-TNAP and *h*-IAP can be selected for further exploration at molecular level.

Disclosure statement

The authors have declared no conflict of interest.

Funding

J. Iqbal is thankful to the Organization for the Prohibition of Chemical Weapons (OPCW), The Hague, The Netherlands and Higher Education Commission, Pakistan for the financial support through Project No. 20-3733/NRPU/R&D/14/520. This work was also supported by Korea Institute of Science and Technology (KIST), KIST Project (E26900).

ORCID

Mohammed I. El-Gamal  <http://orcid.org/0000-0002-4269-5264>

References

- Zimmermann H, Zebisch M, Sträter N. Cellular function and molecular structure of ecto-nucleotidases. *Purinergic Signal* 2012;8:437–502.
- Millán JL. Mammalian alkaline phosphatases: from biology to applications in medicine and biotechnology. Hoboken, NJ, USA: John Wiley & Sons; 2006.
- Millán JL. Alkaline phosphatases: structure, substrate specificity and functional relatedness to other members of a large superfamily of enzymes. *Purinergic Signal* 2006;2:335–41.
- Millán JL. The role of phosphatases in the initiation of skeletal mineralization. *Calcif Tissue Int* 2013;93:299–306.
- Al-Rashida M, Iqbal J. Inhibition of alkaline phosphatase: an emerging new drug target. *Mini Rev Med Chem* 2015;15:41–51.
- Kiffer-Moreira T, Sheen CR, da Silva Gasque KC, et al. Catalytic signature of a heat-stable, chimeric human alkaline phosphatase with therapeutic potential. *PLoS One* 2014;9:e89374.
- Guerville M, Boudry G. Gastrointestinal and hepatic mechanisms limiting entry and dissemination of lipopolysaccharide into the systemic circulation. *Am J Physiol Gastrointest Liver Physiol* 2016;311:G1–G15.
- Buchet R, Millán JL, Magne D. Multisystemic functions of alkaline phosphatases. *Methods Mol Biol* 2013;1053:27–51.
- Yadav MC, Simao AMS, Narisawa S, et al. Loss of skeletal mineralization by the simultaneous ablation of PHOSPHO1 and alkaline phosphatase function: a unified model of the mechanisms of initiation of skeletal calcification. *J Bone Miner Res* 2011;26:286–97.
- Chung TD, Sergienko E, Millán JL. Assay format as a critical success factor for identification of novel inhibitor chemotypes of tissue-nonspecific alkaline phosphatase from high-throughput screening. *Molecules* 2010;15:3010–37.
- Dahl R, Sergienko EA, Su Y, et al. Discovery and validation of a series of aryl sulfonamides as selective inhibitors of tissue-nonspecific alkaline phosphatase (TNAP). *J Med Chem* 2009;52:6919–25.
- Al-Rashida M, Raza R, Abbas G, et al. Identification of novel chromone based sulfonamides as highly potent and selective inhibitors of alkaline phosphatases. *Eur J Med Chem* 2013;66:438–49.
- Salar U, Khan KM, Iqbal J, et al. Coumarin sulfonates: new alkaline phosphatase inhibitors; in vitro and in silico studies. *Eur J Med Chem* 2017;131:29–47.
- Jang HL, El-Gamal MI, Choi HE, et al. Synthesis of tricyclic fused coumarin sulfonates and their inhibitory effects on LPS-induced nitric oxide and PGE₂ productions in RAW 264.7 macrophages. *Bioorg Med Chem Lett* 2014;24:571–5.
- El-Gamal MI, Oh C-H. Synthesis, in vitro antiproliferative activity, and in silico studies of fused tricyclic coumarin sulfonate derivatives. *Eur J Med Chem* 2014;84:68–76.
- El-Gamal MI, Baek D, Oh C-H. A new series of cycloalkane-fused coumarin sulfonates: synthesis and in vitro antiproliferative screening. *Bull Korean Chem Soc* 2016;37:184–91.
- El-Gamal MI, Lee WS, Shin JS, et al. Synthesis of new tricyclic and tetracyclic fused coumarin sulfonate derivatives and their inhibitory effects on LPS-Induced Nitric Oxide and PGE₂ Productions in RAW 264.7 Macrophages: part 2. *Archiv Der Pharmazie* 2016;349:853–63.
- Sergienko EA, Millán JL. High-throughput screening of tissue-nonspecific alkaline phosphatase for identification of effectors with diverse modes of action. *Nat Protoc* 2010;5:1431–9.
- Khan I, Shah SJA, Ejaz SA, et al. Investigation of quinoline-4-carboxylic acid as a highly potent scaffold for the development of alkaline phosphatase inhibitors: synthesis, SAR analysis and molecular modelling studies. *RSC Advances* 2015;5:64404–13.
- Khan I, Ibrar A, Ejaz SA, et al. Influence of the diversified structural variations at the imine functionality of 4-bromophenylacetic acid derived hydrazones on alkaline phosphatase inhibition: synthesis and molecular modelling studies. *RSC Advances* 2015;5:90806–18.
- Molecular Operating Environment (MOE), 2014.09; Chemical Computing Group Inc., 1010 Sherbooke St. West, Suite #910, Montreal, QC, Canada, H3A 2R7, 2015.
- Accelrys Software Inc., Discovery Studio Modeling Environment, Release 4.0, Accelrys Software Inc., San Diego, CA; 2013.
- Li C-J, Chen D-L, Lu Y-Q, et al. Metal-mediated two-atom carbocycle enlargement in aqueous medium. *Tetrahedron* 1998;54:2347–64.
- Woo LWL, Purohit A, Malini B, et al. Potent active site-directed inhibition of steroid sulphatase by tricyclic coumarin-based sulphamates. *Chem Biol* 2000;7:773–91.